

# Improved Quantum State Tomography for Superconducting Quantum Computing Systems

Tao Xin<sup>1,2,\*</sup>

<sup>1</sup>*Shenzhen Institute for Quantum Science and Engineering,  
Southern University of Science and Technology, Shenzhen 518055, China*

<sup>2</sup>*Guangdong Provincial Key Laboratory of Quantum Science and Engineering,  
Shenzhen Institute for Quantum Science and Engineering,  
Southern University of Science and Technology, Shenzhen 518055, Guangdong, China*

Quantum device characterization via state tomography plays an important role in both validating quantum hardware and processing quantum information, unfortunately with the exponential number of the measurements. As one of the main stream quantum platforms, superconducting quantum computing (SQC) system at least requires  $3^n$  measurement settings consisted of single-qubit readout operators in reconstructing a  $n$ -qubit state. In this work, I add the 2-qubit evolutions as the readout operators, and propose an optimal tomographic scheme with the cost-reduced measurements using the integer programming. In detail, I present the minimum number of required measurements to fully reconstruct a state for the Nearest-Neighbor, 2-Dimensional, and All-to-All connectivities on SQC qubits. It is shown that this method can reduce the number of measurements by over 60% compared with the previous state tomography on SQC systems. It is expected that the experimentalist from SQC field can directly utilize the ready-made results for reconstructing quantum states involved in their research. Besides, this method can be applied to reduce the complexity of traditional state tomography in some quantum platforms including but not limited to SQC systems.

## I. INTRODUCTION

For a  $n$ -qubit state,  $4^n - 1$  unknown coefficients are needed to fully describe such a state (with the normalization condition). Quantum state tomography (QST) is the processing of determining these coefficients. In the physical implementations, QST is usually realized by repeatedly measuring the partial information of the state by the measurements on the system, until the complete density matrix of the system is reconstructed [1]. On the one hand, QST being a technique provides us with the results of quantum tasks performed on the quantum systems. On the other hand, QST being a characterization tool is used to benchmark, validate, and develop quantum hardware, which provides an objective indicator in comparing the performance of different quantum devices. Hence, QST has become an indispensable part of quantum information processing [2–4].

Unfortunately, the exponential number of the measurements as the increasing of the size is usually required to finish standard QST [5, 6]. Now, quantum platforms are developing more and more controlled qubits towards larger-scale quantum computing [7]. On SQC systems, the achievements from Google and IBM show that the number of controlled qubits is up to 53 qubits in the laboratory [8] and 16 qubits in quantum cloud computing [9, 10]. In the nuclear magnetic resonance (NMR), they already can control up to 12 qubits by the realization of 12-qubit quantum pseudo-randomness [11]. The photonic quantum computing and ion trap also achieve the control of up to 10 and 14 qubits [12, 13], respectively. So consuming millions of measurements and large amounts of resources are inevitable if we want to perform standard QST on these systems in the future. For instance, performing 8-qubit QST on ion trap required around one week for the measurements and classical post-processing to completely determine a

physical quantum state [14, 15]. In Ref. [16], they spent over two days to estimate a 10-qubit GHZ state on SQC systems, by over  $5.9 \times 10^4$  measurement settings and  $8 \times 10^4$  repeated experiments for each measurement setting. Obviously, the exponentially increasing complexity in QST already hinders the applications of larger-scale quantum processors in exploring quantum advantages.

For a general quantum state in Hilbert space, it is almost impossible to develop a tomographic scheme with the polynomial complexity, but it may be designed and optimized with the fewer measurements. In current quantum platforms, a tomographic process usually contains a series of experiments with different measurement settings, and partial information of the state will be extracted from each experiment. When the obtained information from experiments covers all the unknown coefficients of the state, the density matrix of state will be uniquely reconstructed. However, the obtained information from different measurement settings often overlaps each other. In this case, the key of reducing the complexity of QST is to optimize the tomographic scheme by decreasing redundant measurements as more as possible. The related researches have been made in NMR and optical systems [17, 18]. For some interested quantum states with the restrictions, such as the evolution dynamic and ground states of  $k$ -local Hamiltonian, there may exist some tomographic methods with the polynomial complexity due to the prior information about the state. In the past decades, there have been developed methods for improving the efficiency of QST using some techniques, such as QST via 2-body reduced density matrices [19, 20], compressed sensing [21, 22], machine learning [23–25], matrix product states [5, 6], and parameterized quantum circuits [26, 27].

As the above, there are often overlaps between the partial information obtained from different measurement settings in a tomographic scheme, such that the measured information is usually overcomplete and some measurements are redundant. A natural question is how to find a tomographic scheme with

\* xint@sustech.edu.cn

the minimum number of measurements that still uniquely reconstruct the density matrix of the system. In this work, I investigate this problem by considering 2-qubit evolutions as the options of the readout operators, and find an optimal tomography using the integer programming for SQC systems. Previously, only single-qubit rotations are chosen as the readout operators on SQC systems [16]. Here, I rigorously prove that at least  $3^n$  measurement settings are necessary for determining a state and it is impossible to further reduce the number of measurement settings under single-qubit readout operators. Interestingly, I find that an optimally cost-reduced tomography can be given and the number of measurements can be reduced by over 60% when considering 2-qubit evolutions as the readout operators, in which 2-qubit evolutions refer to the free dynamics of the natural interactions between two qubits and they are easily implemented using the standard techniques on SQC systems. The paper is organized as follows. In Section II, I mainly recall the traditional method of QST on SQC systems and describe the optimal problem of designing the tomographic scheme using the language of the integer programming. In Section III, I present the detailed results of the optimally tomographic schemes with the minimum number of measurements for three different configurations on SQC systems, including the Nearest-Neighbor (NN), 2-Dimensional (2D), and All-to-All (AA) connectivities. Finally, the summary and outlook are presented in Section IV.

## II. TOMOGRAPHIC SCHEME

### A. Problem Description

A general  $n$ -qubit state is fully described by a  $2^n \times 2^n$  density matrix  $\rho$ . Due to the completeness and traceless of the Pauli matrices,  $\rho$  is usually decomposed into the linear combination of the complete Pauli basics with different weights,

$$\rho = \frac{1}{2^n} \mathbb{I}^{\otimes n} + \sum_{i=1}^{4^n-1} \mu_i \mathcal{P}_i, \quad \mu_i = \frac{1}{2^n} \text{Tr}(\rho \mathcal{P}_i). \quad (1)$$

Here,  $\mathbb{I}$  is a  $2 \times 2$  identity operator.  $\mathcal{P}_i$  is a product operator of different Pauli matrices belonging to different qubits. Namely,  $\mathcal{P}_i \in \mathcal{S}_P : \{\mathbb{I}, \mathbb{X}, \mathbb{Y}, \mathbb{Z}\}^{\otimes n}$ , with the Pauli matrices  $\mathbb{X}, \mathbb{Y}, \mathbb{Z}$ .  $\mu_i$  is the expectation value of the operator  $\mathcal{P}_i$ , which is the unknown coefficient to be determined. Equation (1) is a convenient form to measure the desired observables and design the tomographic experiment. In current quantum platforms,  $\mu_i$ 's are often obtained by the different principle of measurement. For instance, as the ensemble, NMR can directly measure the expectation value  $\mu_i$  from experimental spectra [28]. In other platforms, such as SQC and optical systems, the probability distribution in the eigenstates of the operator  $\mathcal{P}_i$  is firstly created by repeating a large amount of experiments and then  $\mu_i$  is computed [29, 30].

There are  $4^n - 1$  of unknown coefficients for a state  $\rho$  to be reconstructed. It is impossible to determine all the coefficients by a kind of measurement setting. Generally speaking,

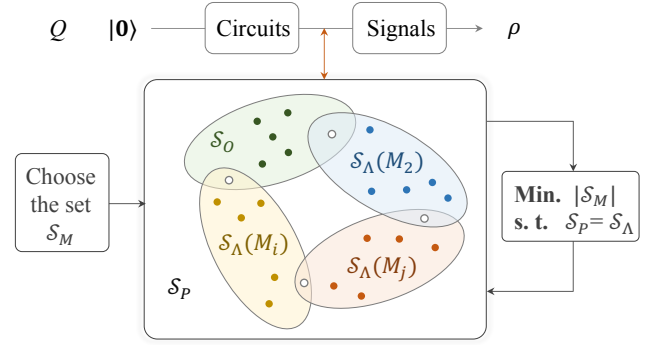


Figure 1. The workflow and schematic diagram for designing a tomographic scheme and reconstructing a state in quantum platforms. The experimentally available set of the measured operators  $\mathcal{S}_O$  is transferred to the set  $\mathcal{S}_\Lambda(M_j)$  under the measurement setting  $M_j \in \mathcal{S}_M$ . Usually, some overlap operators between them (labeled by the white circles) exist. Designing an optimally tomographic scheme is to minimize the number of the set  $\mathcal{S}_M$  (denoted by  $|\mathcal{S}_M|$ ) when the set  $\mathcal{S}_\Lambda \equiv \cup_j \mathcal{S}_\Lambda(M_j)$  covers  $\mathcal{S}_P$ . As a result, the optimized measurement set  $\mathcal{S}_M$  can be implemented between the parts of performing circuits and acquiring signals to reconstruct a state  $\rho$ , with the minimum number of measurements.

a measurement set including different measurement settings is needed in a tomographic experiment. Here, a measurement setting refers to a specific configuration of the detectors (e.g. optical system [31]) or an applied unitary readout operator after performing quantum circuits and before acquiring signals (e.g. SQC [30] and NMR systems [32]). Here, we assume that the set of the experimentally measured operators is  $\mathcal{S}_O = \{O_1, O_2, \dots, O_i, \dots\}$  without any readout operators, and the measurement set including available readout operators is denoted by  $\mathcal{S}_M = \{M_1, M_2, \dots, M_j, \dots\}$ .  $O_i \in \mathcal{S}_P$  is a product operator of Pauli matrices and  $M_j$  is a unitary operation of Clifford group. Under a measurement setting  $M_j \in \mathcal{S}_M$ , the set of experimentally measured operators will be equivalent to  $\mathcal{S}_\Lambda(M_j) = \{\Lambda_1, \Lambda_2, \dots, \Lambda_i, \dots\}$ , with the element  $\Lambda_i = M_j^\dagger O_i M_j$  due to  $\text{Tr}(M_j \rho M_j^\dagger O_i) = \text{Tr}(\rho M_j^\dagger O_i M_j)$ . Obviously,  $\mathcal{S}_\Lambda(M_j) \subseteq \mathcal{S}_P$  for all the readout operators  $M_j \in \mathcal{S}_M$ . When the set  $\mathcal{S}_P$  is completely covered by the set  $\mathcal{S}_\Lambda \equiv \cup_j \mathcal{S}_\Lambda(M_j)$ , the state  $\rho$  will be fully reconstructed. Therefore, there should exist a set  $\mathcal{S}_M$  with the minimum number of elements under the condition that  $\mathcal{S}_P$  is covered by  $\mathcal{S}_\Lambda$ . Figure 1 presents the schematic diagram of the above logic.

Designing and optimizing a tomographic experiment include the following two parts: (i) How to choose the measurement set  $\mathcal{S}_M$  consisted of experimentally available readout operators. It is the premise for us whether reduce the number of measurements QST required. (ii) Under the chosen measurement set  $\mathcal{S}_M$ , how to find a subset of readout operators  $\{M_j\} \subseteq \mathcal{S}_M$  with the minimum number of elements such that the state is fully determined. In the following, I will present the answer behind the above parts for SQC systems.

## B. Traditional QST on SQC Systems

Today, the most used readout method on SQS systems is the so-called dispersive readout [33–35], where each qubit (as quantum system) couples with a readout resonator (as the detector). The Hamiltonian between the qubits and readout resonator can be described by the Jaynes–Cummings model as follows [36],

$$\mathcal{H}_{\text{JC}} = \frac{\omega_0}{2}\sigma_z + g_{0r}(\sigma_+ a + \sigma_- a^\dagger) + \omega_r(a^\dagger a + \frac{1}{2}). \quad (2)$$

Here,  $\omega_0$  and  $\omega_r$  are the frequencies of the qubit and readout resonator, respectively.  $g_{0r}$  is the coupling between the qubit and readout resonator.  $\sigma_x = \mathbb{X}$ ,  $\sigma_y = \mathbb{Y}$ ,  $\sigma_z = \mathbb{Z}$ ,  $\sigma_+ = \sigma_x + i\sigma_y$ , and  $\sigma_- = \sigma_x - i\sigma_y$ . When the qubit is far detuned from the readout resonator with  $\Delta = |\omega_0 - \omega_r| \gg g_{0r}$ , in the dispersive approximation [37], the Hamiltonian can be approximated as

$$\mathcal{H}_{\text{dis}} = \frac{(\omega_0 + g_{0r}^2/\Delta)}{2}\sigma_z + (\omega_r + \frac{g_{0r}^2}{\Delta}\sigma_z)(a^\dagger a + \frac{1}{2}). \quad (3)$$

It is shown that the frequencies of the qubit and readout resonator influence each other, and the states of the qubit lead to a state-dependent frequency shift of the readout resonator. It is  $\omega_r + g_{0r}^2/\Delta$  for the state  $|0\rangle$  or  $\omega_r - g_{0r}^2/\Delta$  for the state  $|1\rangle$ , allowing us to obtain the state information about the qubit by reading the readout resonator. Hence, the probability distributions in the computational basics from  $|00\dots 0\rangle$  to  $|11\dots 1\rangle$  can be measured by repeating a large amount of experiments on SQC systems, corresponding to the measurement of the diagonal elements of the density matrix or the expectation values of the operators in the set  $\{\mathbb{I}, \mathbb{Z}\}^{\otimes n}$ . In this situation, the set of the measured operators  $\mathcal{S}_O$  includes  $2^n$  elements and each operator  $O_i$  belongs to the set  $\{\mathbb{I}, \mathbb{Z}\}^{\otimes n}$ . If we denote  $\mathbb{P}(|\phi_l\rangle)$  as the probability distribution in the  $l$ -th computational basis  $|\phi_l\rangle$ , the expectation value of the operator  $O_i$  is then,

$$\langle O_i \rangle = \frac{1}{2^n} \sum_{l=1}^{2^n} \text{Tr}(O_i \cdot |\phi_l\rangle\langle\phi_l|) \cdot \mathbb{P}(|\phi_l\rangle). \quad (4)$$

It means that  $2^n$  of unknown coefficients in Eq. (1) can be determined by one measurement setting. Hence, at least  $2^n$  of measurement settings are required to fully determine a quantum state for arbitrary set  $\mathcal{S}_M$ . How to choose the set  $\mathcal{S}_M$  is the key of reducing the number of measurement settings. On SQC systems, the applied unitary readout operators acting on each qubit are usually selected from the set  $\{\mathcal{I}, \mathcal{R}_x, \mathcal{R}_y\}$ , where  $\mathcal{I}$  is an identity operator, and  $\mathcal{R}_x \equiv \exp(-i\pi/4\sigma_x)$  and  $\mathcal{R}_y \equiv \exp(-i\pi/4\sigma_y)$  are the  $\pi/2$  rotations around the  $x$  and  $y$  axes, respectively. This corresponds to the measurement set  $\mathcal{S}_M = \{\mathcal{I}, \mathcal{R}_x, \mathcal{R}_y\}^{\otimes n}$  including  $3^n$  of elements. This kind of measurement set has been used on SQC systems. However, I find that  $3^n$  of measurement settings are necessary to fully reconstruct a quantum state under such a set  $\mathcal{S}_M$ , and there does not exist a subset  $\{M_j\} \subseteq \mathcal{S}_M$  such that the state is reconstructed. The rigorous prove is made by means of the recursion theory and it is presented as follows.

*Conclusion 1-*  $3^n$  is the lower bound of the number of measurement settings required to reconstruct a quantum state under  $\mathcal{S}_M = \{\mathcal{I}, \mathcal{R}_x, \mathcal{R}_y\}^{\otimes n}$ .

*Proof-* The set  $\mathcal{S}_P$  is firstly divided into  $(n+1)$  of subsets  $\mathcal{S}_P^{(k)}$ , with  $k$  being the number of Pauli matrices  $\mathbb{X}$  and  $\mathbb{Y}$  in  $\mathcal{P}_i \in \mathcal{S}_P$ .

(i) For the operators  $\mathcal{P}_i \in \mathcal{S}_P^{(0)} : \{\mathbb{I}, \mathbb{Z}\}^{\otimes n}$ , one measurement setting  $\mathcal{I}^{\otimes n}$  is enough to measure  $\mathcal{P}_i$ .

(ii) For the operators  $\mathcal{P}_i \in \mathcal{S}_P^{(1)}$ , there is one Pauli matrix  $\mathbb{X}$  or  $\mathbb{Y}$  in  $\mathcal{P}_i$ , and  $2C_n^1$  of measurement settings where only one qubit occupies  $\mathcal{R}_x$  or  $\mathcal{R}_y$  and the rest qubits occupy  $\mathcal{I}$ 's are needed. For instance, the measurement setting  $\mathcal{R}_x^1 \mathcal{I}^2$  is used to measure the operators  $\mathbb{Y}\mathbb{I}$  and  $\mathbb{Y}\mathbb{Z}$  for a 2-qubit system.

(iii) For the operators  $\mathcal{P}_i \in \mathcal{S}_P^{(2)}$ , there are two Pauli matrices  $\mathbb{X}$  or  $\mathbb{Y}$  in  $\mathcal{P}_i$ , and we need  $2^2 C_n^2$  of measurement settings where only two qubits occupy  $\mathcal{R}_x$  or  $\mathcal{R}_y$  and the rest qubits occupy  $\mathcal{I}$ 's. For example, the measurement setting  $\mathcal{R}_x^1 \mathcal{I}^2 \mathcal{R}_y^3$  is used to measure the operators  $\mathbb{Y}\mathbb{I}\mathbb{X}$  and  $\mathbb{Y}\mathbb{Z}\mathbb{X}$  for a 3-qubit system.

(iv) By that analogy,  $2^n C_n^n$  of measurement settings are needed to measure the operators  $\mathcal{P}_i \in \mathcal{S}_P^{(n)}$ . Totally, the number of required measurement settings is

$$|\mathcal{S}_M|_{\min} = 1 + \sum_{k=1}^n 2^k C_n^k = 3^n. \quad (5)$$

In the following, the above processing for reconstructing a quantum state is called as the standard QST for the comparison with the proposed method in this work.

## C. The New Measurement Settings for QST

Section II B shows that there is not a tomographic scheme whose number of measurements is less than  $3^n$  under the set  $\mathcal{S}_M = \{\mathcal{I}, \mathcal{R}_x, \mathcal{R}_y\}^{\otimes n}$ . In principle, any elements from the Clifford group can be chosen as the unitary readout operators, because the operator  $M^\dagger \mathcal{P}_i M$  also belongs to the set  $\mathcal{S}_P$  under the Clifford operation  $M$  [38]. However, it is not unpractical to consider the entire Clifford group due to the huge size of Clifford group. To find a more efficient QST method on SQC systems, I additionally consider two types of 2-qubit evolutions as the options of the measurement settings, apart from the readout operators  $\mathcal{I}$ ,  $\mathcal{R}_x$ , and  $\mathcal{R}_y$ . They are

$$\mathcal{Y}\mathcal{Y}^{(kl)} \equiv \exp(-i\pi/4\sigma_y^k \sigma_y^l), \quad (6)$$

$$\mathcal{X}\mathcal{Y}^{(kl)} \equiv \exp(-i\pi/4\sigma_x^k \sigma_y^l). \quad (7)$$

$\mathcal{Y}\mathcal{Y}^{(kl)}$  and  $\mathcal{X}\mathcal{Y}^{(kl)}$  are the coupling evolutions between the  $k$ -th and  $l$ -th qubits. On SQC systems, the interaction Hamiltonian between the  $k$ -th and  $l$ -th qubits is  $\mathcal{H}_{\text{int}} = g_{kl}(\sigma_x^k \sigma_x^l + \sigma_y^k \sigma_y^l)$  with the coupling  $g_{kl}$  [16, 39–41], such that  $\mathcal{Y}\mathcal{Y}^{(kl)}$  and  $\mathcal{X}\mathcal{Y}^{(kl)}$  can be easily realized with the assist of the refocusing pulses,

$$\mathcal{Y}\mathcal{Y}^{(kl)} = \exp(-i\mathcal{H}_{\text{int}}\tau) \mathcal{R}_y^k(\pi) \exp(-i\mathcal{H}_{\text{int}}\tau) \mathcal{R}_y^k(-\pi), \quad (8)$$

$$\mathcal{X}\mathcal{Y}^{(kl)} = \mathcal{R}_z^k(-\pi/2) \mathcal{Y}\mathcal{Y}^{(kl)} \mathcal{R}_z^k(\pi/2). \quad (9)$$

Table I. The measured operators when  $\mathcal{Y}\mathcal{Y}^{(kl)}$  and  $\mathcal{X}\mathcal{Y}^{(kl)}$  are chosen as the measurement settings for  $O_i \in \{\mathbb{I}, \mathbb{Z}\}^{\otimes 2}$ .

The operators $O$ 's	$\mathcal{Y}\mathcal{Y}^\dagger O \mathcal{Y}\mathcal{Y}$	$\mathcal{X}\mathcal{Y}^\dagger O \mathcal{X}\mathcal{Y}$
$\mathbb{I}\mathbb{I}$	$\mathbb{I}\mathbb{I}$	$\mathbb{I}\mathbb{I}$
$\mathbb{I}\mathbb{Z}$	$-\mathbb{Y}\mathbb{X}$	$-\mathbb{X}\mathbb{X}$
$\mathbb{Z}\mathbb{I}$	$-\mathbb{X}\mathbb{Y}$	$\mathbb{Y}\mathbb{Y}$
$\mathbb{Z}\mathbb{Z}$	$\mathbb{Z}\mathbb{Z}$	$\mathbb{Z}\mathbb{Z}$

$\tau$  is the free evolution time with the value of  $\tau = \pi/8g_{kl}$ . Then a new measurement set  $\mathcal{S}_M^{\text{new}} = \mathcal{S}_M \cup \mathcal{S}_M^{\text{a}}$  is constructed, including the previous single-qubit set  $\mathcal{S}_M$  and the added two-qubit set  $\mathcal{S}_M^{\text{a}}$ .

$$\mathcal{S}_M^{\text{a}} = \{\mathcal{Y}\mathcal{Y}^{(kl)}, \mathcal{X}\mathcal{Y}^{(kl)}\} \otimes \{\mathbb{I}, \mathcal{R}_x, \mathcal{R}_y\}^{\otimes n-(kl)}. \quad (10)$$

Compared the previous method under the set  $\mathcal{S}_M$ , it is hopeful to find a more efficient tomographic scheme with the number of measurements less than  $3^n$  under the set  $\mathcal{S}_M^{\text{new}}$ . As show in Table I, it is because the introduction of  $\mathcal{Y}\mathcal{Y}^{(kl)}$  and  $\mathcal{X}\mathcal{Y}^{(kl)}$  can measure more non-overlap operators than single-qubit readout operations in the set  $\mathcal{S}_P$ . Now, the question is how to find a subset  $\{M_j\} \subseteq \mathcal{S}_M^{\text{new}}$  with the number of measurement settings as small as possible such that  $\mathcal{S}_\Lambda = \mathcal{S}_P$ . It is a typical set cover problem, but solving the set cover problem is in general NP-hard [42, 43]. Although many famous algorithms are proposed, such as the greedy algorithm, they do not yield the globally optimal solution [44–46].

In this work, I use the integer programming algorithm to find the optimal result for this problem [17, 47]. Let a binary form  $x$  denote a  $|\mathcal{S}_M^{\text{new}}|$ -dimensional column vector, where each element  $x_i$  is zero or one. Only when the  $i$ -th measurement setting  $M_i$  is reserved in the set  $\mathcal{S}_M^{\text{new}}$ , the element  $x_i$  is assigned a value of one. I further denote  $A$  as a  $|\mathcal{S}_M^{\text{new}}| \times 4^N$  sparse matrix, in which the element  $A_{ij} = \text{sgn} \cdot 1$  if  $\mathcal{P}_j \in \mathcal{S}_\Lambda(M_i)$  and zero otherwise, and  $\text{sgn} = \pm 1$  is the plus-minus sign of the corresponding operator in the set  $\mathcal{S}_\Lambda(M_i)$ . In this case, the condition  $\mathcal{S}_\Lambda = \mathcal{S}_P$  is transferred to the linear constraint  $B^T x \geq 1$  with  $B$  being the absolute matrix of  $A$ . Then the objective function of the problem is defined as  $\mathcal{L}(x) = \sum_i x_i$ . Now this problem can be described using the language of the optimization as follows,

$$\text{minimize: } \mathcal{L}(x) = \sum_i x_i \quad (11)$$

$$\text{subject to: } B^T x \geq 1, x_i = 0 \text{ or } 1 \quad (12)$$

Different from general linearly constrained optimization, the above is the binary integer programming. So far, a large collection of algorithms are proposed to solve the integer-programming [48]. In this work, I use the solver Gurobi to find the optimal solution of this problem [49].

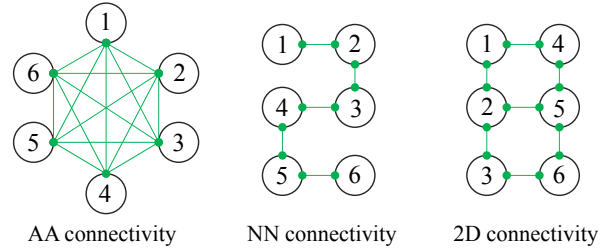


Figure 2. The three common configurations on SQC systems by taking 6-qubit systems as examples.

### III. THE RESULTS AND APPLICATIONS

In this section, I present the results of optimizing the tomographic scheme for three common configurations on SQC systems including the AA, NN, and 2D connectivities in qubits, and the experimentalist can directly utilize the ready-made results for reconstructing quantum states in their researches.

#### A. The AA Configuration

It is known that the connectivity in qubits and the feasibility of two-qubit gates between arbitrary two qubits determine the performance and quality of the performed algorithms on the superconducting chips. Here, I firstly consider the AA configuration on SQC systems. As shown in Fig. 2, it refers to a fully connected graph arrangement of qubits, which is a perfect structure the scientists prefer to develop. For instance, Ref. [16] made a programmable and fully-connected 10-qubit superconducting processor by coupling all the qubits with a bus resonator, in which each qubit can interact with other qubits with the considerable couplings. On such a system, it is available to realize the 2-qubit evolutions  $\mathcal{Y}\mathcal{Y}^{(kl)}$  and  $\mathcal{X}\mathcal{Y}^{(kl)}$  between arbitrary  $k$ -th and  $l$ -th qubits. Now I prove there exists a more efficient tomography with the fewer number of measurement settings compared with standard QST.

Table II. The comparison between standard QST and the proposed tomographic scheme for three common configurations.

Qubit number	2	3	4	5	6	7
Standard QST	9	27	81	243	729	2187
This method-AA	6	15	35	89	265	780
This method-NN	6	16	39	108	293	837
This method-2D	~	~	38	~	284	~

*Conclusion 2-*. Using the proposed tomographic scheme, the number of measurement settings required to reconstruct a quantum state is at least reduced to  $(3^n + 2n + 1)/2$  from the pervious  $3^n$ .

Table III. The optimally tomographic scheme in the measurement set  $\mathcal{S}_M^{\text{new}}$  for the AA configuration. Here, examples of the size with 2 to 4 qubits are presented.

Qubit	Measurement settings
2	$\mathcal{R}_x^2, \mathcal{R}_y^2, \mathcal{R}_x^1, \mathcal{R}_y^1, \mathcal{Y}\mathcal{Y}^{(12)}, \mathcal{X}\mathcal{Y}^{(12)}$
3	$\mathcal{R}_x^2\mathcal{R}_y^3, \mathcal{R}_y^2\mathcal{R}_x^3, \mathcal{R}_x^1\mathcal{R}_y^3, \mathcal{R}_x^1\mathcal{R}_y^2, \mathcal{R}_y^1\mathcal{R}_x^3, \mathcal{R}_y^1\mathcal{R}_x^2, \mathcal{X}\mathcal{Y}^{(12)}, \mathcal{X}\mathcal{Y}^{(12)}\mathcal{R}_x^3, \mathcal{X}\mathcal{Y}^{(12)}\mathcal{R}_y^3, \mathcal{X}\mathcal{Y}^{(13)}, \mathcal{X}\mathcal{Y}^{(13)}\mathcal{R}_x^2, \mathcal{X}\mathcal{Y}^{(13)}\mathcal{R}_y^2, \mathcal{X}\mathcal{Y}^{(23)},$ $\mathcal{R}_x^1\mathcal{X}\mathcal{Y}^{(23)}, \mathcal{R}_y^1\mathcal{X}\mathcal{Y}^{(23)}$
4	$\mathcal{R}_x^3, \mathcal{R}_y^3, \mathcal{R}_x^1\mathcal{R}_x^2\mathcal{R}_x^4, \mathcal{Y}\mathcal{Y}^{(12)}, \mathcal{X}\mathcal{Y}^{(12)}, \mathcal{Y}\mathcal{Y}^{(12)}\mathcal{R}_y^4, \mathcal{X}\mathcal{Y}^{(12)}\mathcal{R}_x^3\mathcal{R}_x^4, \mathcal{Y}\mathcal{Y}^{(12)}\mathcal{R}_x^3\mathcal{R}_y^4, \mathcal{Y}\mathcal{Y}^{(12)}\mathcal{R}_y^3\mathcal{R}_x^4, \mathcal{X}\mathcal{Y}^{(12)}\mathcal{R}_y^3\mathcal{R}_y^4, \mathcal{Y}\mathcal{Y}^{(13)}, \mathcal{X}\mathcal{Y}^{(13)},$ $\mathcal{Y}\mathcal{Y}^{(13)}\mathcal{R}_x^4, \mathcal{X}\mathcal{Y}^{(13)}\mathcal{R}_y^4, \mathcal{X}\mathcal{Y}^{(13)}\mathcal{R}_x^2, \mathcal{Y}\mathcal{Y}^{(13)}\mathcal{R}_y^2, \mathcal{Y}\mathcal{Y}^{(14)}, \mathcal{X}\mathcal{Y}^{(14)}, \mathcal{Y}\mathcal{Y}^{(14)}\mathcal{R}_x^2\mathcal{R}_x^3, \mathcal{X}\mathcal{Y}^{(14)}\mathcal{R}_x^2\mathcal{R}_y^3, \mathcal{Y}\mathcal{Y}^{(14)}\mathcal{R}_y^2, \mathcal{X}\mathcal{Y}^{(14)}\mathcal{R}_y^2\mathcal{R}_x^3,$ $\mathcal{Y}\mathcal{Y}^{(14)}\mathcal{R}_y^2\mathcal{R}_y^3, \mathcal{Y}\mathcal{Y}^{(23)}\mathcal{R}_x^4, \mathcal{X}\mathcal{Y}^{(23)}\mathcal{R}_y^4, \mathcal{R}_x^1\mathcal{Y}\mathcal{Y}^{(23)}, \mathcal{R}_y^1\mathcal{X}\mathcal{Y}^{(23)}, \mathcal{Y}\mathcal{Y}^{(24)}, \mathcal{X}\mathcal{Y}^{(24)}, \mathcal{R}_x^1\mathcal{Y}\mathcal{Y}^{(24)}, \mathcal{R}_y^1\mathcal{X}\mathcal{Y}^{(24)},$ $\mathcal{R}_x^2\mathcal{X}\mathcal{Y}^{(34)}, \mathcal{R}_y^2\mathcal{Y}\mathcal{Y}^{(34)}, \mathcal{R}_x^1\mathcal{X}\mathcal{Y}^{(34)}, \mathcal{R}_y^1\mathcal{Y}\mathcal{Y}^{(34)}$

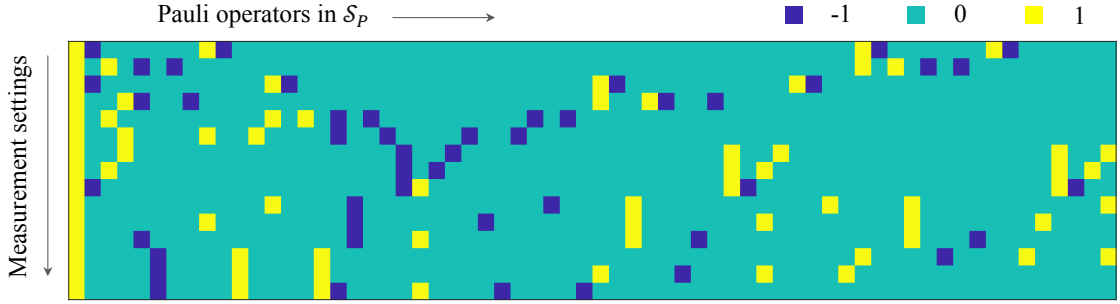


Figure 3. The values of the optimal matrix  $A^t$  after removing the redundant measurement settings for a 3-qubit AA configuration. It is a  $15 \times 64$  matrix, in which the horizontal axis is the index of 64 Pauli operators  $\mathcal{P}_i \in \{\mathbb{I}\mathbb{I}\mathbb{I}, \mathbb{I}\mathbb{I}\mathbb{X}, \dots, \mathbb{Z}\mathbb{Z}\mathbb{Z}\}$  and the vertical axis is the index of 15 measurement settings shown in Table III.  $A_{ij}^t = \pm 1$  refers to the Pauli operator  $\mathcal{P}_j$  can be measured in the  $i$ -th measurement setting. Here,  $-1$  is the sign of the corresponding measured Pauli operator.

*Proof.* Similar with the derivation in Section II B, the set  $\mathcal{S}_P$  is divided into  $\mathcal{S}_P = \mathcal{S}_P^{(0)} \cup \mathcal{S}_P^{(1)} \cup \dots \cup \mathcal{S}_P^{(N-1)} \cup \mathcal{S}_P^{(N)}$ .

(i) For the operators  $\mathcal{P}_i \in \mathcal{S}_P^{(0)} : \{\mathbb{I}, \mathbb{Z}\}^{\otimes n}$ , one measurement setting  $\mathcal{I}^{\otimes n}$  is still used to measure  $\mathcal{P}_i$ .

(ii) For measuring the operators  $\mathcal{P}_i \in \mathcal{S}_P^{(1)}$ , we need  $2C_n^1$  of single-qubit measurement settings where only one qubit occupies  $\mathcal{R}_x$  or  $\mathcal{R}_y$  and the rest qubits occupy  $\mathcal{I}$ 's.

(iii) For the operators  $\mathcal{P}_i \in \mathcal{S}_P^{(2)}$ , there are two Pauli matrices  $\mathbb{X}$  or  $\mathbb{Y}$  in  $\mathcal{P}_i$ . We need  $2 \cdot C_n^2$  of measurement settings where only two qubits are  $\mathcal{Y}\mathcal{Y}^{(kl)}$  or  $\mathcal{X}\mathcal{Y}^{(kl)}$  and the rest qubits are  $\mathcal{I}$ 's. For instance, the measurement setting  $\mathcal{Y}\mathcal{Y}^{(12)}\mathcal{I}^3$  is capable to measure the operators  $\mathbb{Y}\mathbb{X}\mathbb{I}$ ,  $\mathbb{Y}\mathbb{X}\mathbb{Z}$ ,  $\mathbb{X}\mathbb{Y}\mathbb{I}$ , and  $\mathbb{X}\mathbb{Y}\mathbb{Z}$  for a 3-qubit system.

(iv) For the operators  $\mathcal{P}_i \in \mathcal{S}_P^{(3)}$ , there are three Pauli matrices  $\mathbb{X}$  or  $\mathbb{Y}$  in  $\mathcal{P}_i$ . We need  $2 \cdot 2 \cdot C_n^3$  of measurement settings where two qubits occupy  $\mathcal{Y}\mathcal{Y}^{(kl)}$  or  $\mathcal{X}\mathcal{Y}^{(kl)}$ , one qubit occupies  $\mathcal{R}_x$  or  $\mathcal{R}_y$ , and the rest qubits occupy  $\mathcal{I}$ 's. For instance, the measurement setting  $\mathcal{Y}\mathcal{Y}^{(12)}\mathcal{I}^3\mathcal{R}_x^4$  is capable to measure the operators  $\mathbb{Y}\mathbb{X}\mathbb{I}\mathbb{Y}$ ,  $\mathbb{Y}\mathbb{X}\mathbb{Z}\mathbb{Y}$ ,  $\mathbb{X}\mathbb{Y}\mathbb{I}\mathbb{Y}$ , and  $\mathbb{X}\mathbb{Y}\mathbb{Z}\mathbb{Y}$  for a 4-qubit system.

(v) By that analogy,  $2 \cdot 2^{n-2} \cdot C_n^n$  of measurement settings are necessary to measure the operators  $\mathcal{P}_i \in \mathcal{S}_P^{(n)}$ . The first fac-

tor of 2 is due to two selections from  $\mathcal{Y}\mathcal{Y}^{(kl)}$  or  $\mathcal{X}\mathcal{Y}^{(kl)}$  and the second factor of 2 means two selections from  $\mathcal{R}_x$  or  $\mathcal{R}_y$ . Totally, the number of required measurement settings is

$$1 + 2C_n^1 + \sum_{k=2}^n 2^{k-1} C_n^k = \frac{3^n + 2n + 1}{2}. \quad (13)$$

It is worth stressing that the above result in Eq. (13) is not the optimal solution of this problem. Next, I use the binary integer programming to find the optimal result. For the AA configuration,  $|\mathcal{S}_M^{\text{new}}| = 3^n + 3^{n-2} \cdot 2 \cdot C_n^2$  due to the full connectivity in qubits. As shown in Table II, the minimum number of measurement settings is presented as a function of qubit number. The complexity of QST is reduced to 780 from 2187 with saving over 64% of measurements for a 7-qubit system. In Table III, I provide some examples of the required measurement settings to reconstruct a  $n$ -qubit state for  $n = 2, 3, 4$ . I also plot the thin matrix  $A^t$  after removing the redundant measurement settings from the matrix  $A$  in Fig. 3.  $A^t$  is a more convenient form for the experimentalist to perform state tomography and recover the density matrix according to the experimental data.

Table IV. The optimally tomographic scheme in the measurement set  $\mathcal{S}_M^{\text{new}}$  for the NN configuration. Here, examples of the size with 2 to 4 qubits are presented.

Qubit	Measurement settings
2	$\mathcal{R}_x^2, \mathcal{R}_y^2, \mathcal{R}_x^1, \mathcal{R}_y^1, \mathcal{Y}\mathcal{Y}^{(12)}, \mathcal{X}\mathcal{Y}^{(12)}$
3	$\mathcal{R}_x^2, \mathcal{R}_x^2\mathcal{R}_x^3, \mathcal{R}_y^2, \mathcal{R}_y^2\mathcal{R}_y^3, \mathcal{R}_x^1\mathcal{R}_x^3, \mathcal{R}_x^1\mathcal{R}_y^3, \mathcal{R}_x^1\mathcal{R}_x^2, \mathcal{R}_y^1\mathcal{R}_x^3, \mathcal{R}_y^1\mathcal{R}_y^3, \mathcal{R}_y^1\mathcal{R}_y^2, \mathcal{Y}\mathcal{Y}^{(12)}, \mathcal{Y}\mathcal{Y}^{(12)}\mathcal{R}_x^3, \mathcal{X}\mathcal{Y}^{(12)}\mathcal{R}_x^3, \mathcal{Y}\mathcal{Y}^{(23)},$ $\mathcal{R}_x^1\mathcal{X}\mathcal{Y}^{(23)}, \mathcal{R}_y^1\mathcal{Y}\mathcal{Y}^{(23)}$
4	$\mathcal{R}_x^2\mathcal{R}_x^4, \mathcal{R}_x^2\mathcal{R}_y^4, \mathcal{R}_x^2\mathcal{R}_y^3, \mathcal{R}_y^2\mathcal{R}_x^4, \mathcal{R}_y^2\mathcal{R}_y^4, \mathcal{R}_y^2\mathcal{R}_x^3, \mathcal{R}_x^1\mathcal{R}_x^4, \mathcal{R}_x^1\mathcal{R}_y^4, \mathcal{R}_x^1\mathcal{R}_x^3, \mathcal{R}_x^1\mathcal{R}_y^3, \mathcal{R}_y^1\mathcal{R}_x^4, \mathcal{R}_y^1\mathcal{R}_y^4, \mathcal{R}_y^1\mathcal{R}_x^3, \mathcal{R}_y^1\mathcal{R}_y^3, \mathcal{Y}\mathcal{Y}^{(12)}\mathcal{R}_x^4,$ $\mathcal{X}\mathcal{Y}^{(12)}\mathcal{R}_x^4, \mathcal{Y}\mathcal{Y}^{(12)}\mathcal{R}_y^4, \mathcal{X}\mathcal{Y}^{(12)}\mathcal{R}_y^4, \mathcal{Y}\mathcal{Y}^{(12)}\mathcal{R}_x^3, \mathcal{X}\mathcal{Y}^{(12)}\mathcal{R}_x^3, \mathcal{X}\mathcal{Y}^{(12)}\mathcal{R}_x^3\mathcal{R}_x^4, \mathcal{Y}\mathcal{Y}^{(12)}\mathcal{R}_x^3\mathcal{R}_y^4, \mathcal{Y}\mathcal{Y}^{(12)}\mathcal{R}_y^3, \mathcal{X}\mathcal{Y}^{(12)}\mathcal{R}_y^3, \mathcal{Y}\mathcal{Y}^{(12)}\mathcal{R}_y^3\mathcal{R}_x^4,$ $\mathcal{X}\mathcal{Y}^{(12)}\mathcal{R}_y^3\mathcal{R}_y^4, \mathcal{X}\mathcal{Y}^{(23)}, \mathcal{X}\mathcal{Y}^{(23)}\mathcal{R}_x^4, \mathcal{Y}\mathcal{Y}^{(23)}\mathcal{R}_y^4, \mathcal{R}_x^2\mathcal{Y}\mathcal{Y}^{(34)}, \mathcal{R}_y^2\mathcal{X}\mathcal{Y}^{(34)}, \mathcal{R}_x^1\mathcal{Y}\mathcal{Y}^{(34)}, \mathcal{R}_y^1\mathcal{X}\mathcal{Y}^{(34)},$ $\mathcal{R}_x^1\mathcal{R}_x^2\mathcal{Y}\mathcal{Y}^{(34)}, \mathcal{R}_x^1\mathcal{R}_y^2\mathcal{X}\mathcal{Y}^{(34)}, \mathcal{R}_y^1\mathcal{Y}\mathcal{Y}^{(34)}, \mathcal{R}_y^1\mathcal{X}\mathcal{Y}^{(34)}, \mathcal{R}_y^1\mathcal{R}_x^2\mathcal{X}\mathcal{Y}^{(34)}, \mathcal{R}_y^1\mathcal{R}_y^2\mathcal{Y}\mathcal{Y}^{(34)}$

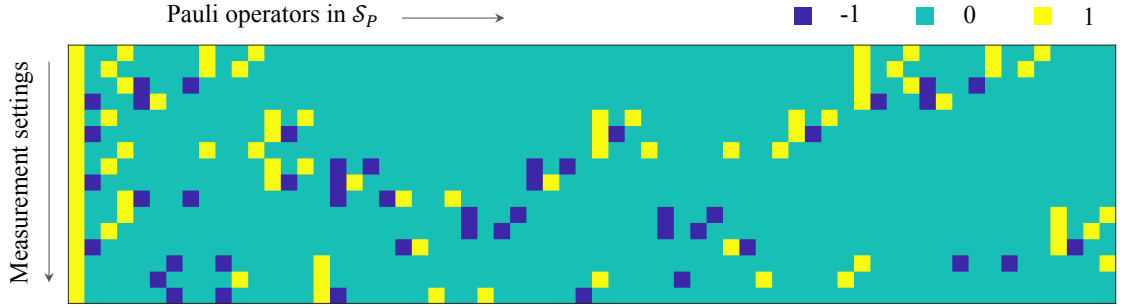


Figure 4. The values of the optimal matrix  $A^t$  after removing the redundant measurement settings for a 3-qubit NN configuration. It is a  $16 \times 64$  matrix, in which the horizontal axis is the index of 64 Pauli operators  $\mathcal{P}_i \in \{\text{III}, \text{IX}, \dots, \text{ZZZ}\}$  and the vertical axis is the index of 16 measurement settings shown in Table IV.  $A_{ij}^t = \pm 1$  refers to the Pauli operator  $\mathcal{P}_j$  can be measured in the  $i$ -th measurement setting. Here,  $-1$  is the sign of the corresponding measured Pauli operator.

## B. The NN and 2D Configurations

Considering that the challenge of developing the AA configuration in practice, I further study the optimization of the tomographic scheme for the more common NN and 2D configurations. As shown in Fig. 2, the NN connectivity in qubits is a natural arrangement on a linear array of qubits, in which two-qubit operations are only available on the nearest-neighbor qubits. Many famous superconducting chips developed on SQC systems adopt this structure. For instance, the 5-qubit and 9-qubit NN superconducting chips arranged in a linear array were developed with the direct coupling in Ref. [50–52]. In Table II, I present the optimal number of measurement settings required for a  $n$ -qubit chain with  $n$  from 2 to 7. The corresponding measurement settings are provided in Table IV. Figure 4 shows the optimal matrix  $A^t$  by taking a 3-qubit chain as an example. The 2D configuration is another chip structure where each qubit can couple with the surrounding qubits, such as the SQC chips from Google and IBM teams [8–10], and a two-by-two planar lattice of SQC qubits [53]. As test examples, I find the minimum number of measurement settings using the integer programming for 4-qubit and 6-qubit 2D structures and they are also shown in Table II. Due to the higher connectivity in qubits, the AA configura-

tion has the fewer measurement settings than the NN and 2D configurations for fully reconstructing a quantum state.

## IV. DISCUSSION AND CONCLUSION

In summary, I study how to reduce the number of measurement settings when the measured information is enough to determine a quantum state and attempt to optimize this problem by the integer programming. Finally, I propose a closed-loop solution for the experimentalist to reconstruct a quantum state on SQC systems, with the higher efficiency than the standard QST used, and some numerical examples are presented for three common configurations in qubits. It may be a little hard to use the binary integer programming to find the optimally tomographic scheme for a larger quantum system, but it is still easy to find a suboptimal solution or approximate solution for the intermediate-scale quantum systems. In this work, I assume that one measurement setting includes at most one 2-qubit evolution. Actually, if we consider more 2-qubit evolutions or select other elements from Clifford group, the minimum number of measurement settings will be further reduced. To boost the speed of finding the optimal solution via the integer programming, the symmetry of this problem

should be taken into account. For instance, there are some symmetries in the sets  $\mathcal{S}_P$ ,  $\mathcal{S}_O$ , and  $\mathcal{S}_M$ . If these symmetries are considered in using the integer programming algorithms, the computation amount of reaching the optimal solution is likely reduced [54], which is an interesting question for the tomography in the larger systems in the future research. The results obtained in this work can be applied to some quantum platforms including but not limited to SQC systems, and the ideas and methods developed in this work will be also helpful in designing the feasible tomographic experiments in practice.

## ACKNOWLEDGMENTS

This work was supported by the National Natural Science Foundation of China (No. U1801661 and No. 11905099), Guangdong Basic and Applied Basic Research Foundation (Grant No. 2019A1515011383), and Guangdong Provincial Key Laboratory (Grant No.2019B121203002).

- 
- [1] P. Busch, *International Journal of Theoretical Physics* **30**, 1217 (1991).
- [2] M. Baur, A. Fedorov, L. Steffen, S. Filipp, M. P. da Silva, and A. Wallraff, *Phys. Rev. Lett.* **108**, 040502 (2012).
- [3] A. I. Lvovsky and M. G. Raymer, *Rev. Mod. Phys.* **81**, 299 (2009).
- [4] A. Erhard, J. J. Wallman, L. Postler, M. Meth, R. Stricker, E. A. Martinez, P. Schindler, T. Monz, J. Emerson, and R. Blatt, *Nat. Commun.* **10**, 1 (2019).
- [5] M. Cramer, M. B. Plenio, S. T. Flammia, R. D. Somma, D. Gross, S. D. Bartlett, O. Landoncardinal, D. Poulin, and Y. Liu, *Nat. Commun.* **1**, 149 (2010).
- [6] B. P. Lanyon, C. Maier, M. Holzzapfel, T. Baumgratz, C. Hempel, P. Jurcevic, I. Dhand, A. S. Buyskikh, A. J. Daley, M. Cramer, *et al.*, *Nat. Phys.* **13**, 1158 (2017).
- [7] L. Gyongyosi and S. Imre, *Comput. Sci. Rev.* **31**, 51 (2019).
- [8] F. Arute, K. Arya, R. Babbush, D. Bacon, J. C. Bardin, R. Barends, R. Biswas, S. Boixo, F. G. S. L. Brandao, D. A. Buell, *et al.*, *Nature* **574**, 505 (2019).
- [9] J. R. Wootton and D. Loss, *Phys. Rev. A* **97**, 052313 (2018).
- [10] Y. Wang, Y. Li, Z. Yin, and B. Zeng, *Npj Quantum Inf.* **4**, 46 (2018).
- [11] J. Li, Z. Luo, T. Xin, H. Wang, D. Kribs, D. Lu, B. Zeng, and R. Laflamme, *Phys. Rev. Lett.* **123**, 030502 (2019).
- [12] H. Wang, Y. He, Y. Li, Z. Su, B. Li, H. Huang, X. Ding, M. Chen, C. Liu, J. Qin, *et al.*, *Nat. Photonics* **11**, 361 (2017).
- [13] T. Monz, P. Schindler, J. T. Barreiro, M. Chwalla, D. Nigg, W. A. Coish, M. Harlander, W. Hänsel, M. Hennrich, and R. Blatt, *Phys. Rev. Lett.* **106**, 130506 (2011).
- [14] H. Haffner, W. Hansel, C. F. Roos, J. Benhelm, D. Chekalkar, M. Chwalla, T. Korber, U. D. Rapol, M. Riebe, P. O. Schmidt, *et al.*, *Nature* **438**, 643 (2005).
- [15] A. B. Klimov, C. Muñoz, A. Fernández, and C. Saavedra, *Phys. Rev. A* **77**, 060303 (2008).
- [16] C. Song, K. Xu, W. Liu, C.-p. Yang, S.-B. Zheng, H. Deng, Q. Xie, K. Huang, Q. Guo, L. Zhang, P. Zhang, D. Xu, D. Zheng, X. Zhu, H. Wang, Y.-A. Chen, C.-Y. Lu, S. Han, and J.-W. Pan, *Phys. Rev. Lett.* **119**, 180511 (2017).
- [17] J. Li, S. Huang, Z. Luo, K. Li, D. Lu, and B. Zeng, *Phys. Rev. A* **96**, 032307 (2017).
- [18] G. M. Leskowitz and L. J. Mueller, *Phys. Rev. A* **69**, 052302 (2004).
- [19] N. Linden and W. K. Wootters, *Phys. Rev. Lett.* **89**, 277906 (2002).
- [20] T. Xin, D. Lu, J. Klassen, N. Yu, Z. Ji, J. Chen, X. Ma, G. Long, B. Zeng, and R. Laflamme, *Phys. Rev. Lett.* **118**, 020401 (2017).
- [21] C. Riofrío, D. Gross, S. T. Flammia, T. Monz, D. Nigg, R. Blatt, and J. Eisert, *Nat. Commun.* **8**, 1 (2017).
- [22] D. Ahn, Y. S. Teo, H. Jeong, F. Bouchard, F. Hufnagel, E. Karimi, D. Koutný, J. Řeháček, Z. Hradil, G. Leuchs, and L. L. Sánchez-Soto, *Phys. Rev. Lett.* **122**, 100404 (2019).
- [23] G. Torlai, B. Timar, E. P. L. van Nieuwenburg, H. Levine, A. Omran, A. Keesling, H. Bernien, M. Greiner, V. Vuletić, M. D. Lukin, R. G. Melko, and M. Endres, *Phys. Rev. Lett.* **123**, 230504 (2019).
- [24] A. M. Palmieri, E. V. Kovlakov, F. Bianchi, D. Yudin, S. S. Straupe, J. Biamonte, and S. P. Kulik, *Npj Quantum Inf.* **6**, 1 (2019).
- [25] T. Xin, S. Lu, N. Cao, G. Anikeeva, D. Lu, J. Li, G. Long, and B. Zeng, *Npj Quantum Inf.* **5**, 1 (2019).
- [26] T. Xin, X. Nie, X. Kong, J. Wen, D. Lu, and J. Li, *Phys. Rev. Applied* **13**, 024013 (2020).
- [27] Y. Liu, D. Wang, S. Xue, A. Huang, X. Fu, X. Qiang, P. Xu, H.-L. Huang, M. Deng, C. Guo, X. Yang, and J. Wu, *Phys. Rev. A* **101**, 052316 (2020).
- [28] L. M. K. Vandersypen and I. L. Chuang, *Rev. Mod. Phys.* **76**, 1037 (2005).
- [29] P. Krantz, A. Bengtsson, M. Simoen, S. Gustavsson, V. Shumeiko, W. Oliver, C. Wilson, P. Delsing, and J. Bylander, *Nat. Commun.* **7**, 1 (2016).
- [30] P. Krantz, M. Kjaergaard, F. Yan, T. P. Orlando, S. Gustavsson, and W. D. Oliver, *Appl. Phys. Rev.* **6**, 021318 (2019).
- [31] K. Sanaka, K. Kawahara, and T. Kuga, *Phys. Rev. Lett.* **86**, 5620 (2001).
- [32] D. G. Cory, A. F. Fahmy, and T. F. Havel, *Proc. Natl. Acad. Sci.* **94**, 1634 (1997).
- [33] M. Naghiloo, *arXiv preprint arXiv:1904.09291* (2019).
- [34] S. Filipp, P. Maurer, P. J. Leek, M. Baur, R. Bianchetti, J. M. Fink, M. Göppl, L. Steffen, J. M. Gambetta, A. Blais, and A. Wallraff, *Phys. Rev. Lett.* **102**, 200402 (2009).
- [35] T. Walter, P. Kurpiers, S. Gasparinetti, P. Magnard, A. Potočnik, Y. Salathé, M. Pechal, M. Mondal, M. Oppliger, C. Eichler, and A. Wallraff, *Phys. Rev. Applied* **7**, 054020 (2017).
- [36] B. W. Shore and P. L. Knight, *J. Mod. Opt.* **40**, 1195 (1993).
- [37] A. Blais, R.-S. Huang, A. Wallraff, S. M. Girvin, and R. J. Schoelkopf, *Phys. Rev. A* **69**, 062320 (2004).
- [38] J. Dehaene and B. De Moor, *Phys. Rev. A* **68**, 042318 (2003).
- [39] R. Barends, J. Kelly, A. Megrant, D. Sank, E. Jeffrey, Y. Chen, Y. Yin, B. Chiaro, J. Mutus, C. Neill, P. O'Malley, P. Roushan, J. Wenner, T. C. White, A. N. Cleland, and J. M. Martinis, *Phys. Rev. Lett.* **111**, 080502 (2013).
- [40] Y. Chen, C. Neill, P. Roushan, N. Leung, M. Fang, R. Barends, J. Kelly, B. Campbell, Z. Chen, B. Chiaro, A. Dunsworth, E. Jeffrey, A. Megrant, J. Y. Mutus, P. J. J. O'Malley, C. M. Quintana, D. Sank, A. Vainsencher, J. Wenner, T. C. White, M. R. Geller, A. N. Cleland, and J. M. Martinis, *Phys. Rev. Lett.* **113**, 220502 (2014).

- [41] A. Niskanen, K. Harrabi, F. Yoshihara, Y. Nakamura, S. Lloyd, and J. S. Tsai, *Science* **316**, 723 (2007).
- [42] E. Halperin and R. M. Karp, *Theor. Comput. Sci.* **348**, 240 (2005).
- [43] N. Alon, B. Awerbuch, and Y. Azar, in *Proceedings of the thirty-fifth annual ACM symposium on Theory of computing* (2003) pp. 100–105.
- [44] R. Hassin and A. Levin, *SIAM J. Comput.* **35**, 189 (2005).
- [45] R. Bar-Yehuda and S. Even, *J. Algorithms* **2**, 198 (1981).
- [46] N. E. Young, *Encyclopedia of algorithms*, 379 (2008).
- [47] A. Schrijver, *Theory of linear and integer programming* (John Wiley & Sons, 1998).
- [48] D. Chen, R. Batson, and Y. Dang, “Applied integer programming: modeling and solution. 2011,”.
- [49] *Gurobi Solver*, <https://www.gurobi.com>.
- [50] W. Cai, J. Han, F. Mei, Y. Xu, Y. Ma, X. Li, H. Wang, Y. P. Song, Z.-Y. Xue, Z.-q. Yin, S. Jia, and L. Sun, *Phys. Rev. Lett.* **123**, 080501 (2019).
- [51] R. Barends, J. Kelly, A. Megrant, A. Veitia, D. Sank, E. Jeffrey, T. C. White, J. Mutus, A. G. Fowler, B. Campbell, *et al.*, *Nature* **508**, 500 (2014).
- [52] J. Kelly, R. Barends, A. G. Fowler, A. Megrant, E. Jeffrey, T. C. White, D. Sank, J. Y. Mutus, B. Campbell, Y. Chen, *et al.*, *Nature* **519**, 66 (2015).
- [53] A. D. Córcoles, E. Magesan, S. J. Srinivasan, A. W. Cross, M. Steffen, J. M. Gambetta, and J. M. Chow, *Nat. Commun.* **6**, 1 (2015).
- [54] F. Margot, in *50 Years of Integer Programming 1958-2008* (Springer, 2010) pp. 647–686.